Appl Phys B (2010) 101: 71–74
DOI 10.1007/s00340-010-4149-9

Applied Physics B
Lasers and Optics

Diode end-pumped acousto-optically Q-switched compact Nd:YLF laser

V. Besotosnii · E. Cheshev · M. Gorbunkov · P. Kostryukov · M. Krivonos · V. Tunkin · D. Jakovlev

Received: 9 February 2010 / Revised version: 15 May 2010 / Published online: 27 July 2010

Abstract Compact diode end-pumped acousto-optically Q-switched Nd:YLF laser was developed. As in effective CW diode end-pumped lasers, pump beam was made sufficiently narrower than resonator Gaussian mode to increase efficiency in Q-switched operation. The dramatic changes of output radiation structure were observed at some resonator lengths. The radiation structure is close to the Gaussian mode in intervals between these lengths.

1 Introduction

The diode end-pumping of solid-state lasers offers the possibility to achieve high quality laser beams with high efficiency. For this purpose, the pump beam dimensions should be made smaller than the Gaussian mode diameter [1, 2]. In this case, the radiation spatial structures (RSS) of the CW laser depend on the resonator length L [3–6]. It can be dramatically far from the Gaussian mode at some degenerate L, determined by the expression

$$\arccos(g_1 g_2)^{1/2} = \pi r/s, \tag{1}$$

where r/s is an irreducible fraction, $g_{1,2} = 1 - L/R_{1,2}$ are resonator parameters, $R_{1,2}$ are radii of mirror curvatures. It was shown in [7] that the degenerate condition (1) is not sufficient to form the radiation with complicated structure and thus to create critical configurations; it is necessary to use also narrow enough pump beams. This fact was demonstrated in experiments with Nd:YVO_4, Nd:YAG and Nd:YLF CW lasers [3–6, 8, 9].

Q-switched compact diode end-pumped lasers DEPL are important sources for a wide range of applications: Doppler LIDAR and remote sensing [10], precise micromachining of diamond [11], laser spark plugs [12], grooving and scribing [13], laser cutting [14] and so on. Typical energies per pulse were 1–15 mJ and typical repetition rates 1–50 kHz. Repetition rate of 500 kHz was achieved in [14]. Passively Q-switched compact DEPL were developed in [15–20]. Dependence of the output RSS on L was not discussed in any paper devoted to active or passive Q-switched DEPL [10–20]. The question is: What are the manifestations of Q-switched DEPL spatial structure dependence on L?

The use of the pump beam narrower than zero-order Gaussian mode can be useful to increase efficiency only when AM thermal lensing is relatively weak. Nd:YLF has a sufficiently weak thermal lensing which makes it an ideal crystal to investigate RSS as a function of L.

In this work, compact acousto-optically Q-switched Nd:YLF diode end-pumped laser with near-Gaussian mode was developed. To achieve higher efficiency, pump beam dimensions were made sufficiently smaller than the Gaussian mode diameter. The dependence of the output radiation spatial structure on resonator length was investigated.

2 Experimental setup

The experimental setup of an acousto-optically Q-switched Nd:YLF DEPL is shown in Fig. 1. A thermostabilized CW laser diode LD of 4 W maximum power emitting at

V. Besotosnii · E. Cheshev · M. Gorbunkov · M. Krivonos
P.N. Lebedev Physical Institute, Russian Academy of Sciences, Leninski prospect 53, Moscow, 119991, Russia

P. Kostryukov · V. Tunkin (✉) · D. Jakovlev
M.V. Lomonosov Moscow State University, International Laser Center and Faculty of Physics, Leninskie Gory, Moscow, 119991, Russia
e-mail: vgtunkin@mail.ru

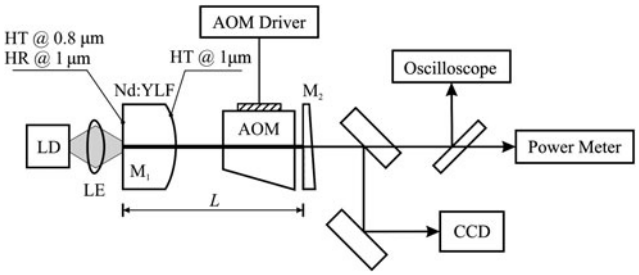

Fig. 1 Experimental setup of diode end-pumped acousto-optically Q-switched Nd:YLF laser: *LD*—laser diode, *LE*—focusing lens, M_1—end mirror, *AOM*—acousto-optical modulator, M_2—output coupler with 75% reflection at laser wavelength of 1.047 μm

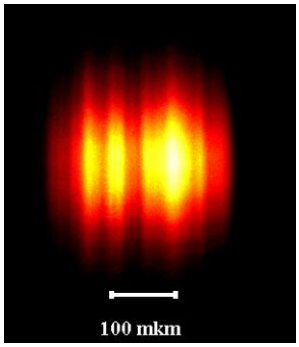

Fig. 2 Pump beam spatial structure, measured by CCD camera at M_1

0.805 μm is used as a pump source. The cylindrical lens with a focal length of 0.5 mm reduces pump beam divergence along LD fast axis. A lens LE of 4.24 mm focal length focuses LD output to spot dimensions $S \approx 0.15$ mm × 0.21 mm (on the level of 0.5 intensity) onto a 6 mm-long and 4 mm-diameter Nd:YLF active medium AM. The optical axis of AM is perpendicular to the resonator axis. AM is inserted inside a copper block heat sink using heat conducting hermetic. The plain side of AM facing the pump beam is antireflection coated at the pump wavelength and reflection coated at the laser wavelength of 1.047 μm (mirror M_1). The other side of AM has radius of curvature 60 mm and is antireflection coated for the laser wavelength. Output coupler is a plane mirror M_2 with 75% reflection at the laser wavelength. It is mounted on the translation stage that offers the possibility to scan L continuously to observe the resonator critical and noncritical configurations. The plane-concave geometry of AM and the use of plane OC allow to change resonator length by moving OC without resonator misalignment. Moreover, plane wavefront just before OC gives possibility to install nonlinear crystal for intracavity second harmonic generation or other angle-sensitive element inside the resonator. For this reason, such schemes are used in compact single-diode pumped lasers [21].

A compact acousto-optical modulator AOM is placed inside the resonator. An RF driver of 8 W power working at 80 MHz produces in quartz crystal a running acoustic wave AW of 10 mm length along resonator axis and of 1 mm width in the region of intersection with the laser beam. A resonator Gaussian mode has diameter of ∼0.4 mm at M_1. Pump beam measured by a CCD camera at M_1 is shown in Fig. 2.

The output RSS were recorded by CCD camera. The total path between M_2 and CCD camera was 320 mm. A pair of plane-parallel plates decreases an energy falling on CCD camera. The radiation power was measured by a power-meter FieldMaster with measuring head LM-10. Q-switched pulse shape was monitored by Tektronix DPO-4032.

3 Results and discussion

The time of acoustic wave passing through laser beam T_P and the switching time of RF driver define the time of resonator Q-factor triggering T_Q. The diameter of the Gaussian mode of our compact laser is ∼0.3 mm; the speed of acoustic wave in quartz is 5970 m/s, so T_P is equal to ∼50 ns. Taking into account the switching time of RF driver, T_Q is increased on several tenths of nanoseconds compared to T_P. The roundtrip time of our laser is 0.55 ns, thus the process of resonator Q-factor triggering goes on for more than 100 roundtrip times. This time is comparable with the time of RSS formation of fundamental resonator mode. Therefore, it can be expected that RSS dependences on L of acousto-optically Q-switched and CW effective compact lasers have the same features.

As L was scanned, the dramatic changes of RSS were observed in Q-switched operation at the critical configurations $r/s = 1/3, 3/10, 1/4, 1/5, 1/6, 1/8$ (1). RSS of the ring type were observed at this critical configurations and at absorbed pump power P not higher than 1.5 W. Such ring structures should be observed in the critical configurations even of astigmatic resonators in the case of sufficiently short resonators with output coupler of sufficiently low reflectivity [9].

At $P > 2$ W, ring structures transform at high enough repetition rates into the stretched ones as in critical configuration $r/s = 1/4$ (Fig. 3c, d, e) due to the anisotropy of active medium thermal properties. Corresponding RSS are shown in Fig. 3 for two resonator configurations: critical $r/s = 1/4$ (Fig. 3a, b, c, d, e), noncritical (Fig. 3f, g, h, i, j), and for several operating modes: AW is running continuously (AOM closed, Fig. 3a, f); Q-switched with repetition rates $f = 1$ kHz (Fig. 3b, g), 3 kHz (Fig. 3c, h), and 20 kHz (Fig. 3d, i); AW is cut off—CW operation is realized (Fig. 3e, j).

Concrete lengths corresponding to the critical configurations depend on P and S due to the influence of the thermal lens. The resonator length $L_1 = 69.5$ mm (Fig. 3a, b, c, d, e, $P = 2.4$ W, $S \approx 0.15$ mm × 0.21 mm) is approximately in the center of the critical configuration $r/s = 1/4$

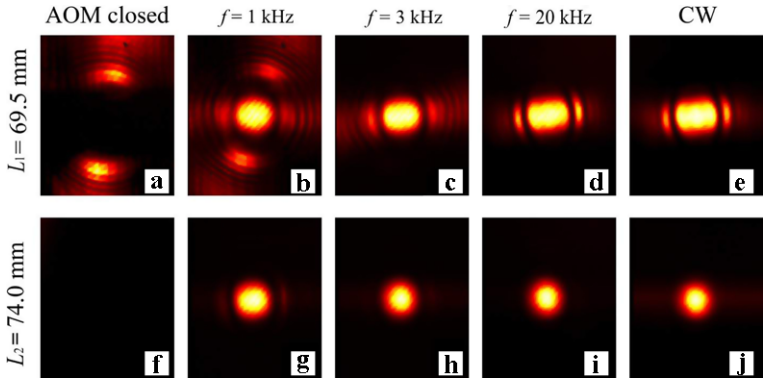

Fig. 3 Output radiation spatial structures for two resonator configurations: critical $r/s = 1/4$ at $L_1 = 69.5$ mm (**a**, **b**, **c**, **d**, **e**), noncritical at $L_2 = 74.0$ mm (**f**, **g**, **h**, **i**, **j**), and for several operating modes: acoustic wave is running continuously (AOM closed) (**a**, **f**); Q-switched with repetition rates $f = 1$ kHz (**b**, **g**), 3 kHz (**c**, **h**) and 20 kHz (**d**, **i**); acoustic wave is cut off—CW operation is realized (**e**, **j**)

corresponding to the semiconfocal and at the same time dynamically stable resonator [22]. RSS at this critical configuration is the most complicated [7]. As the repetition rate was increased, RSS transformed close to the superposition of Hermite–Gaussian modes observed in CW operation (Fig. 3e). In Q-switched operation, RSS at repetition rates over at least 3 kHz and at noncritical configurations become close to the Gaussian mode (Fig. 3g, h, i). The resonator length difference between neighboring critical configurations $r/s = 1/4$ and $r/s = 3/10$ is for our laser ~22 mm. As L is scanned in the interval of ~12 mm inside noncritical configuration situated between these critical configurations, RSS remain close to the Gaussian mode.

When AW is running continuously (AOM closed), the laser generates at $r/s = 1/4$ (Fig. 3a) as well as in other critical configurations, but no generation is observed at noncritical configurations (Fig. 3f). Closed AOM has sufficiently low transmission only near resonator axis due to the finite width of AW (1 mm). Laser radiation passes round AW at AOM off-axis regions. In Fig. 3a (AOM closed) one can clearly see the horizontal dark stripe in the center of the pattern. This dark stripe corresponds to the on-axis region of AOM low transmission. We have observed RSS at various distances from OC and have found that laser radiation consists at semiconfocal configuration from four rays with different angles in a vertical plane. These so-called geometrical modes [23] are possible only in the case of the degenerate resonator configurations [24]. We have found that output power of geometrical modes (AOM closed) is ~60% of output power in CW operation at semiconfocal configuration $r/s = 1/4$. This means that up to several tenths percent of power may be lost in Q-switched operation at critical configurations and low repetition rates. RSS in Q-switched operation at critical configuration $r/s = 1/4$ and repetition rate $f = 1$ kHz is shown in Fig. 3b. The central spot in this figure corresponds to Q-switched pulse, and radiation in peripheral area corresponds to geometrical modes generated in time intervals when AOM is closed.

The problem of dynamical stability of resonators was discussed in [22]. As it can be seen from [22], for dynamically stable resonators and for thermal lens situated sufficiently close to one of the mirrors (M_1 in our case), $dw_1/df = 0$, where w_1 is the spot radius on this mirror, f is the thermal lens focal length, but $dw_2/df \neq 0$, where w_2 is the spot radius on output coupler M_2. The feature of many types of DEPL is that the thermal lens is adjacent to the end mirror M_1 (not to the output coupler). It can be easily shown using relations given, for example, in [22] that for a thin thermal lens the minimum of dw_2/df is reached at $g_1 = 0.375 (g_2 = 1)$. From this point of view, the length of the resonator with minimum of dw_2/df should be somewhat longer than the length of the semiconfocal resonator ($g_1 = 0.5$, $g_2 = 1$).

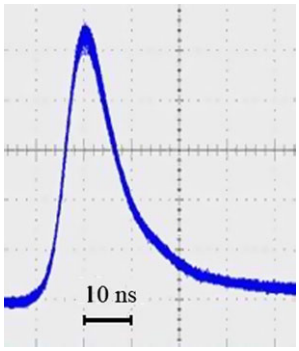

Fig. 4 Q-switched pulse shape at resonator noncritical configurations

Q-switched pulse shape at noncritical configurations where RSS are close to the Gaussian mode is shown in Fig. 4. Duration of the pulse at 1 kHz repetition rate is 9 ns, at 3 kHz is 12 ns. The average output power at 3 kHz repetition rate is 0.8 W, at 20 kHz is 1.4 W at 2.4 W of absorbed power.

The optimization of the acousto-optically Q-switched compact Nd:YLF diode end-pumped laser with radiation structure close to the Gaussian mode was implemented. To achieve higher efficiency, the pump beam dimensions were made sufficiently smaller than the diameter of the resonator Gaussian mode. It was shown that spatial radiation structure is far from the Gaussian one at certain degenerate resonator lengths. It was shown also that at these lengths the considerable distortions of the spatial structure are caused not only

by superposition of cold resonator modes as in CW lasers but also by acousto-optical modulator due to so-called geometrical modes existing only in degenerate resonators. The most considerable distortions were observed near degenerate length corresponding to semiconfocal resonator. A few-millimeter detuning from this length allowed us to obtain the best radiation spatial structure close to the Gaussian mode, and at the same time to conserve low influence of the thermal lens on the output beam size. Thus, an effective acousto-optically Q-switched compact diode end-pumped Nd:YLF laser with radiation structure close to the Gaussian mode was developed.

Acknowledgements This work was supported by the Russian Foundation for Basic Research (Grant Nos. 08-08-00108-a, 08-02-12143-ofi and 09-02-01190-a) and the program of the fundamental research of the Department of Physical Sciences RAS "Fundamental Problems of Photonics and Physics of New Optical Materials".

References

1. P. Laporta, M. Brussard, IEEE J. Quantum Electron. **27**, 2319 (1991)
2. F. Sanches, M. Brunel, K. Ait-Ameur, J. Opt. Soc. Am. B **15**, 2390 (1998)
3. H.-H. Wu, C.-C. Sheu, T.-W. Chen, M.-D. Wei, W.-F. Hsieh, Opt. Commun. **165**, 225 (1999)
4. C.-H. Chen, P.-T. Tai, W.-F. Hsieh, J. Opt. Soc. Am. B **20**, 1220 (2003)
5. J. Frauchiger, P. Alhers, H.P. Weber, IEEE J. Quantum Electron. **28**, 1046 (1992)
6. G. Martel, C. Labbe, F. Sanches, M. Frimager, K. Ait-Ameur, Opt. Commun. **201**, 117 (2002)
7. M.V. Gorbunkov, P.V. Kostryukov, V.G. Tunkin, Quantum Electron. **38**, 689 (2008)
8. V.V. Bezotosnyi, E.A. Cheshev, M.V. Gorbunkov, P.V. Kostryukov, V.G. Tunkin, Appl. Opt. **47**, 3651 (2008)
9. V.V. Bezotosnyi, M.V. Gorbunkov, P.V. Kostryukov, V.G. Tunkin, E.A. Cheshev, D.V. Jakovlev, Quantum Electron. **39**, 759 (2009)
10. H. Zhang, P. Shi, D. Li, K. Du, Appl. Opt. **42**, 1681 (2003)
11. S.K. Sudheer, V.P. Mahadevan Pillai, V.U. Nayar, J. Optoelectron. Adv. Mater. **8**, 363 (2006)
12. D.L. McIntyre, S.D. Woodruff, J.S. Ontko, in *Internal Combustion Engine Spring Technical Conference*, May 3–6, 2009, Wisconsin. www.asmeconference.org
13. A. Pauchard, K. Lee, N. Vago, M. Pavius, S. Obi, www.synova.ch/pdf/2009
14. X. Fu, Q. Liu, X. Yan, J. Cui, M. Gong, Appl. Phys. B **95**, 63 (2009)
15. Z. Quan, Z. Ling, Ye Ziqing, T. Huiming, Q. Longshend, Opt. Lasers Technol. **33**, 355 (2001)
16. Z. Hong, H. Zheng, J. Chen, J. Ge, Appl. Phys. B **73**, 205 (2001)
17. L. Lv, L. Wang, P. Fu, X. Chen, Z. Zhang, V. Gaebler, D. Li, B. Liu, H.J. Eichler, S. Zhang, A. Liu, Z. Zhu, Opt. Lett. **26**, 72 (2001)
18. Y. Kalisky, L. Kravchik, C. Labbe, Opt. Commun. **189**, 113 (2001)
19. A. Agnesi, S. Dell Acqua, Appl. Phys. B **76**, 351 (2003)
20. S.P. Ng, D.Y. Tang, L.J. Quin, X.L. Meng, Opt. Commun. **229**, 331 (2004)
21. V.V. Bezotosnyi, N.F. Glushenko, I.D. Zalevski, Ju.M. Popov, V.P. Semenkov, E.A. Cheshev, Quantum Electron. **35**, 507 (2005)
22. J.P. Lörtscher, J. Steffen, G. Herziger, Opt. Quantum Electron. **7**, 505 (1975)
23. I.A. Ramsay, J.J. Degnan, Appl. Opt. **9**, 385 (1970)
24. J. Dingjan, M.P. van Exter, J.P. Woerdman, Opt. Commun. **188**, 345 (2001)